Journal of Thermal Analysis and Calorimetry, Vol. 73 (2003) 577–586

CRYSTALLIZATION AND GLASS PROPERTIES OF PENTITOLS
Xylitol, adonitol, arabitols

L. Carpentier[*]*, S. Desprez and M. Descamps*

Laboratoire de Dynamique et Structure des Matériaux Moléculaires, U.M.R. CNRS 8024, Bât. P5, Ust Lille, 59655 Villeneuve d'Ascq, France

Abstract

Thermodynamic and dynamic data of the four pentitols, xylitol, adonitol, *l*-arabitol and *d*-arabitol, measured by Temperature Modulated DSC (TMDSC) in the crystalline and amorphous states are presented. The properties of the supercooled liquids clearly show two distinct kinds of thermal behaviors with regard to their aptitude to crystallize. The capacity of the TMDSC technique to characterize both the molecular mobility and the thermal behavior is used to analyze the stability of the supercooled liquid state of the compounds. The comparison between the pentitols shows that the crystallization processes are mainly dominated by the interfacial energy rather than by a competition between the thermodynamic driving force and the molecular mobility.

Keywords: crystallization, fragility index, glass transition, molecular mobility, pentitol, specific heat spectroscopy

Introduction

Actual and future developments of therapeutic agents are highly concerned by the duality 'crystalline state/amorphous state' of drug substances and excipients. The solid form is, in pharmaceutical industry, a privileged route to elaborate medicines due to its greater stability in regard to the liquid form, considering physical and chemical stability. Typically and traditionally, new drug candidates enter the pharmaceutical development process in the crystalline form which is the most stable solid state. However this state of lowest energy is also the less soluble. The actual technical challenges concerning the new therapeutic development aim to control these two antagonist features to optimize formulations. From this point of view the amorphous state, while considered as less stable, offers some interesting attractive potentialities in the control of the bioavailability [1–3]. The two important physical problems to address in this context are:

- The characterization of the temperature dependence of the molecular mobility of the amorphous state. This property is directly related to the glass formation of the

* Author for correspondence: E-mail: Laurent.Carpentier@univ-lille1.fr

1388–6150/2003/ $ 20.00
Akadémiai Kiadó, Budapest

compound and to the evolution of the different transport coefficients. It is through the temperature dependence of these transport coefficients that the glass formers are classified, according their so-called degree of fragility [4, 5].

• The stability of the amorphous state with regard to recrystallization. Conventionally this transformation is understood as resulting of a nucleation and growth process of the more stable state. Their occurrence and kinetics are the result of a delicate balance between the thermodynamic driving force and the molecular mobility.

The Temperature Modulated DSC (TMDSC) is a new technique which provides both thermodynamic and molecular dynamic information on a system. We use this technique to discuss the glass formation and recrystallization tendency of a family of conformational isomers, namely xylitol, adonitol, *l*-arabitol and *d*-arabitol. The Fisher projections of these pentitols of general formula $CH_2OH–(CHOH)_3-CH_2OH$ are:

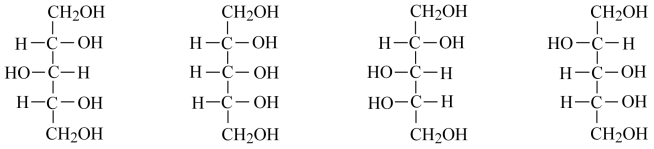

a) Xylitol b) Adonitol c) l-arabitol d) d-arabitol

Scheme 1

One objective of this study is to get information on the effects which are not only dependent on the molecular mass. TMDSC offers the possibility to perform a specific heat spectroscopy in the course of one temperature scan and to access the complex heat capacity $C^*_\omega(T)$ [8, 9]. TMDSC covers a frequency domain of one decade in the range 0.01 to 0.1 Hz which allows us to investigate the dynamics of glass-forming liquids just above the glass transformation domain. Although this domain is narrow, it is sufficient to obtain an estimation of the slope $\left|\mathrm{d}\log\tau/\mathrm{d}(T_g/T)\right|_{T=T_g}$, directly related to the fragility index *m* [10, 11]. The paper is organized as follows: the specific heat spectroscopic capability of the technique and the main signals corresponding to this technique are presented in the first section. In the second section, TMDSC is used as a standard DSC to characterize the thermal behavior of the four pentitols. In the third section a kinetic investigation of the pentitols is presented. These data as a whole are compared and discussed in the fourth section in order to determine the origin of the propensity to crystallize of the different pentitols.

TMDSC signals

The theoretical basis and the description of the TMDSC signals of a specific heat spectroscopy are presented in detail in several papers to which the reader can refer [8, 10–12]. We summarized in this section the main characteristics of these signals. With this technique, a periodic modulation of temperature at pulsation ω is superimposed on the normal linear temperature ramp (rate *q*). The modulated temperature sweeping rate is given by:

$$\dot{T}(t) = q + \dot{T}_0 \cos(\omega t) \tag{2}$$

with $\dot{T}_0 = A\omega$, where A is the amplitude of the temperature modulation. TMDSC experiments are completely defined by the 3 experimental parameters A, q and ω. The accessible frequency range of the calorimeter lies in the 1/10–1/100 s^{-1} range. It allows to detect enthalpic resonances in the glass transition region [10, 11]. In the case we are far from any irreversible reaction of the system (such as crystallization), the resulting heat flow can be written as:

$$\dot{Q} = qC_p(q,t) + \dot{Q}_0 \cos(\omega t - \phi) \tag{3}$$

where the first term is the usual DSC signal at q rate and the second term corresponds to the additional modulated response. From the determination of this latter quantity and the modulated temperature rate, we can derive a phase lag ϕ and a complex, frequency dependent, specific heat capacity modulus $\left|C^*_\omega(T)\right|$ defined by:

$$\left|C^*_\omega(T)\right| = \frac{\dot{Q}_0}{\dot{T}_0} \tag{4}$$

$$C^*_\omega(T) = \left|C^*_\omega(T)\right| e^{i\phi} \tag{5}$$

Examples of these different signals obtained on xylitol and recorded when scanning the glass transformation range upon cooling are displayed in Fig. 1a. The characteristic features of the approach of the glass transition shown by this measurement (Fig. 1b) are:

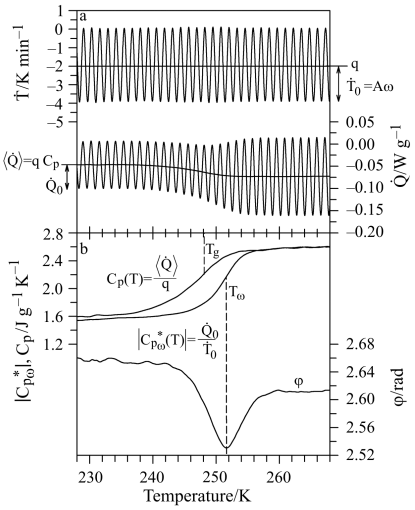

Fig. 1 a – Temperature evolution of the main TMDSC signals obtained on xylitol: the modulated temperature $\dot{T}$, and modulated heat flow $\dot{Q}$. The experimental parameters are q=–2 K min^{-1}, A=0.212 K and $\omega/2\pi$=1/40 s^{-1} ('cool only' conditions); b – The signals which are used to determine the complex heat capacity $C^*_\omega(T)$ are calculated from $\dot{T}$, and $\dot{Q}$

– The conventional heat capacity jump occurring at T_g, associated to the underlying linear cooling rate (q=–2 K min^{-1}).

– The frequency dependent jump of the modulated heat flow amplitude $\dot{Q}_0$, occurring at a temperature somewhat higher T_ω. T_g and T_ω reveal different ergodicity breaking temperatures associated to the different time scales of the two dynamic perturbations q and ω.

– A peak in the phase lag φ at T_ω.

The magnitude of the phase lag is critical to the evaluation of the real C'_ω and imaginary C''_ω parts of the complex heat capacity. It is argued that the phase angle should be 0 in the supercooled liquid and glassy regions (which is not the case in Fig. 1b). The origin of a non-zero phase angle results from several contributions that are related to experimental and to intrinsic properties of the material. These contributions are essentially due to heat transfers from the calorimeter to the sample, which are strongly dependent on thermal contacts between sample and calorimeter, and heat conductivity of the sample itself. As a consequence, baseline corrections are necessary to get the usable phase lag. It has been shown [11, 13] that the baseline can be constructed by scaling $|C^*_\omega(T)|$ such that it matches the measured phase angle in the metastable and glassy regions. $C^*_\omega(T)$ is separated into a real (in phase) $C'_\omega(T)$ and imaginary (out of phase) $C''_\omega(T)$ component, using the corrected phase lag ϕ_{cor}:

$$C'_\omega(T) = \left|C^*_\omega\right| \cos\phi_{cor} \tag{6}$$

$$C''_\omega(T) = \left|C^*_\omega\right| \sin\phi_{cor} \tag{7}$$

The phase lag exhibits a continuous shift of the peak maximum (T_ω) towards higher temperatures when the modulation frequency increases. In an other way, the peak position is not influenced by the underlying rate q. These observations clearly reveal the relaxational origin of the phase peak. The signals are then used to extract dynamic information just above the glass transition temperature.

Thermal behavior of pentitols

Standard and modulated differential scanning calorimetry were performed using the TA Instruments 2920 TMDSC in conjunction with a refrigerated cooling system (RCS). Standard DSC was used to measure the temperature and enthalpy of crystallization and fusion of the different samples. The calorimeter head was flushed with a highly pure helium gas. The baseline was calibrated by scanning the temperature domain with an empty pan. The temperature and enthalpy readings were calibrated with respect to the melting point of pure indium. The four pentitols, obtained from Aldrich Chemical Company Inc., were used without further purification. They were encapsulated in aluminum crimped pans. The sample mass was in the range of 5–10 mg which is a low enough value to allow the sample to follow the imposed thermal oscillations [10]. All the standard DSC scans were performed at a heating rate of 5 K min^{-1}.

Table 1 Thermal characteristics of the pentitols obtained from the melting of the crystalline powders (T_m, ΔH_m, ΔS_m) and after reheating the quenched liquid (T_g, T_c, χ)

	T_m/K	ΔH_m/ kJ mol^{-1}	ΔS_m/ J mol^{-1} K^{-1}	T_c/K	χ/%	T_g/K
Xylitol	368	37.7	102	n.c.	–	250
Adonitol	375	33.5	89	349	38	252
l-Arabitol	374	43.2	115	n.c.	–	261
d-Arabitol	376	38.8	103	348	91	261

The purpose of the first heating sequence (Fig. 2 - curves A) was the melting of the crystalline powders of the different pentitols. After melting, the compounds were quenched by a rapid cooling (≈30 K min^{-1}) below their respective glass transition temperature. During the second heating sequence (Fig. 2 - curves B), the shape of the DSC curves was widely different depending on the type of pentitols analyzed. Whereas xylitol and *l*-arabitol exhibited only a well-defined glass transition corresponding to a C_p increase, the thermal behavior of adonitol and *d*-arabitol (observed in the same thermal treatment conditions) was more complex. In addition to the characteristic C_p jump at T_g, both compounds are characterized by the presence of an exothermic cold crystallization peak located just before the melting peak. The melting enthalpies corresponding to the second heating ramp are lower than those obtained during the first heating ramp. It indicates that, at q=5 K min^{-1}, the compounds are not fully crystallized before melting. The ratio of the first and second heating enthalpies allows to determine the rate of crystallization. The glass transition temperature T_g, the melting enthalpy ΔH_m, the melting entropy ΔS_m, the melting temperatures T_m, the crystallization temperature T_c, as well as the transformed fraction χ of the four

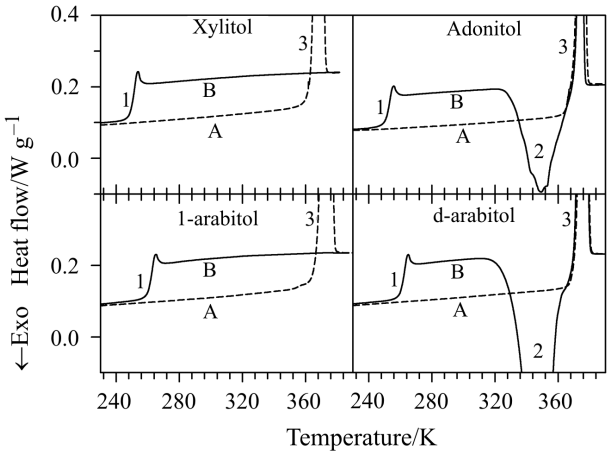

Fig. 2 Typical DSC traces obtained at a 5 K min^{-1} scanning rate. Curves A (dashed lines): first heating to remove crystalline phase, curves B (solid lines): second heating after quenching below T_g. The different events are: 1 – glass transition; 2 – cold crystallization; 3 – melting

pentitols are reported in Table 1. Since crystallization and melting are closed for adonitol and *d*-arabitol, the temperatures of the two thermal events are determined from the peak maximum. The glass transition temperature is determined in regard to the midpoint of the C_p jump.

Molecular mobility of pentitols

TMDSC signals, recorded when scanning the glass transformation range upon cooling, are obtained by repeated temperature scans around T_g, using the underlying cooling rate q=–0.1 K min^{-1}, at various frequencies in the range (1/10–1/100 s^{-1}). The amplitude and frequency were chosen so that the amplitude of the modulated temperature rate is kept constant for each experiment: $\dot{T}_0 = A\omega = \pi/100$. Since xylitol and *l*-arabitol do not crystallize, even at low cooling rates, the spectroscopy measurements for these two compounds are performed without further melting of the samples. On the other hand, for adonitol and *d*-arabitol, the sequence: heating up to the melting temperature – quench to bypass the crystallization, is repeated before each measurement. The low sweeping rate value, q= –0.1 K min^{-1}, minimizes possible 'levelling effects' responsible for an unphysical decrease of the C''_ω amplitude when frequency decreases [10]. This effect, observed for high q values, becomes preponderant when the two following processes are in competition: the sample falling out of the equilibrium at a temperature $T_g(q)$ associated to the underlying cooling rate q giving rise to the classical $C_p(q)$ drops, and the glass transition at $T_g(\omega)$ associated to the characteristic time of the modulated temperature identifiable by $C''_\omega(T)$ drops. It has been shown [10] that, for such low cooling rates the data are reversible and correspond thus to the equilibrium metastable liquid.

Dynamic information can be determined from the real $C''_\omega(T)$ and imaginary $C''_\omega(T)$ parts (Figs 3a and 3b) of the complex heat capacity $C''_\omega(T)$ measured between 1/100 and 1/20 s^{-1}. The temperature of the enthalpy loss maximum T_ω at constant frequency $\omega/2\pi$ varies strongly with ω. It corresponds to the temperature where the characteristic relaxation time of the sample $\tau(T_\omega)=1/\omega$ is the most probable. Figure 4 shows the relaxation times measured for the four pentitols, on a log scale, *vs*. T_g/T for five different periods of modulation (20 to 100 s). The glass transition temperatures of the linear ramp T_g (Table 1) correspond to the relaxation time extrapolated to the temperature for which $\tau(T_g)$=100 s. TMDSC thus probes the structural relaxation mechanism which is arrested at T_g on the experimental time scale and corresponds to the α–relaxation process. As expected for the narrow covered frequency/temperature range, the evolution of the relaxation times follows an Arrhenius behavior:

$$\tau(T) = \tau_0 \exp\left(-\frac{E}{T_\omega}\right) \tag{8}$$

where E is an energy barrier (expressed in Kelvin) and τ_o a characteristic time.

Nevertheless, the very large activation energies (summarized in Table 2) indicate that the overall evolution of the dynamic must be strongly non-Arrhenius. Attempt to analyze the temperature evolution of this process using a Vogel–Tamman–Fülcher (V.F.T.) equation is hampered by the impossibility to cover many decades of frequency on the

high temperature side of the plot. Nevertheless it is possible to calculate the slope of the relaxation time measured at T_g and to determine the fragility parameter m defined by:

$$m=\left|\frac{\mathrm{d}\log\tau}{\mathrm{d}(T_g/T)}\right|_{T=T_g}=\frac{E}{T_g(\tau=100\ \mathrm{s})\ln(10)} \tag{9}$$

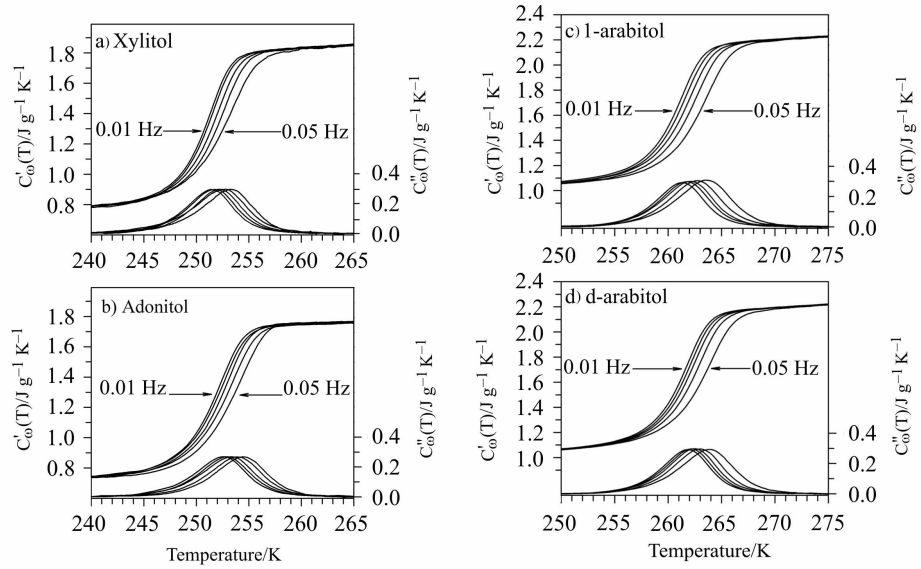

Fig. 3 Real and imaginary parts of the complex specific heat $C^*_\omega(T)$ of a – xylitol, b – adonitol, c – *l*-arabitol and d – *d*-arabitol, as a function of temperature on cooling (q=–0.1 K min^{-1}). The curves refer to periods of the modulated temperature 100–20 s in steps of 20 s, in the order of increasing temperature

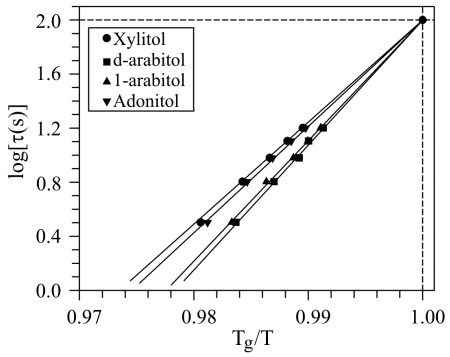

Fig. 4 Enthalpic relaxation times evolution of the four pentitols in a log scale as a function of the reciprocal temperature. The full lines are the results of a fit with an Arrhenius law. The glass transition temperature T_g corresponds to the temperature when mean relaxation time is 100 s

The results of the refinements on the Arrhenius law are gathered together in Fig. 4. In regard to the strong limit $m \approx 16$ corresponding to a thermally activated process, the four pentitols are fragile liquids.

Table 2 Kinetic characteristics of the pentitols from the specific heat spectroscopy analysis. T_g is determined by extrapolation of the relaxation time to τ=100 s

	E/K	$\log(\tau_0)$ $[\tau_0/s^{-1}]$	$T_g(\tau=100\ s)$/ K	ΔC_p/ J g^{-1} K^{-1}	Fragility index, m
Xylitol	43532	–74	250	1.14	76±3
Adonitol	44854	–76	251	1.16	78±3
l-Arabitol	53237	–87	259	1.35	90±3
d-Arabitol	54974	–90	259	1.35	92±3

Discussion and conclusions

The analysis of the thermal behavior of the four pentitols revealed important differences with regard to their aptitude to crystallize. Subjected to the thermal treatments described in the second section, the pair xylitol/*l*-arabitol does not crystallize upon reheating, contrary to the pair adonitol/*d*-arabitol. These observations lead to analyze the kinetics of the metastable state decay in the frame of a nucleation and growth mechanism. In the simplest case, infinitesimal super-critical droplets of stable phase appear randomly at constant rate J per unit volume. This stage is followed by an isotropic grain growth with a constant linear velocity V. Classical nucleation theory [14–15] gives the following expression for the steady state nucleation rate:

$$J(T)=J_0 \exp\left(-\frac{E'}{T}\right)\exp\left(-\frac{\Delta G^*}{T}\right) \tag{10}$$

where the prefactor J_0 is weakly temperature dependent.

It is often assumed that E' is close to the activation energy of the transport coefficients (diffusion and/or viscosity) associated with the crossing of the liquid-solid interface. ΔG^* is the energy barrier required to form a critical size nucleus. ΔG^* can be expressed in terms of the Gibbs free energy difference between the two phases and the corresponding interface energy γ [16]:

$$\Delta G^* \propto \frac{\gamma^3}{\Delta G_v^2} \tag{11}$$

For a polymorphic transformation, the growth is expected to be linear with time:

$$V(T)=V_0 \exp\left(-\frac{E'}{T}\right)\left(1-\exp\left[-\frac{v\Delta G_v}{T}\right]\right) \quad (v\text{: molecular volume}) \tag{12}$$

For a given compound (assuming a fixed value of γ), both expressions (10, 12) predict a competition between the thermodynamic driving force and the molecular mobility. TMDSC gives some possibilities to estimate and discuss the relative influence of the two contributions. At temperatures $T<T_m$ the Gibbs free energy difference between the metastable liquid and the crystalline phases is given by:

$$\Delta G_v = \Delta S_m (T - T_m) - \int_T^{T_m} dT \int_T^{T_m} \frac{\Delta C_p}{T} dT \quad (13)$$

The higher limit value of E ($\equiv E'$) near T_g is also provided by TMDSC as it has been shown above. Figure 5 shows the temperature dependence of the thermodynamic driving force for the four pentitols deduced from the present calorimetric data (in the evaluation, ΔC_p has been assumed to be constant). The confrontation with the aptitude to crystallize of the different compounds shows that the thermodynamic driving force can not explain these behaviors: *l*-arabitol, which does not crystallize upon heating, possesses the highest driving force value whereas adonitol, with the lowest driving force value, crystallizes upon heating. Another parameter governing the crystallization processes is the activation energy E. Increasing E lowers the nucleation rate and raises the temperature at which the nucleation rate becomes maximum. As shown in Fig. 4, there is no more logical link between the aptitude to crystallize and the values of the transport coefficient activation energy. As a consequence, only a noticeable difference between the value of liquid–crystal surface energies, related to the specific molecular conformations of the different compounds, allows to explain the origin of the different crystallization behaviors of the four pentitols. Another way to describe the ability of adonitol and *d*-arabitol to crystallize is to consider not a homogenous but a heterogeneous nucleation mechanism. In that case, a better crystallization tendency is also governed by the interfacial tension value. The confrontation of the present results with a calorimetric analysis of hexitols (characterized by a linear chain of 6 carbon atoms) [17] reveals a clear different origin of the crystallization

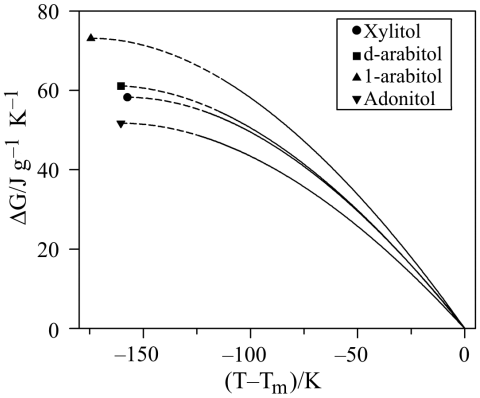

Fig. 5 Temperature dependence of the differences in Gibbs free energy between the supercooled liquid and the crystalline phases. Full lines: normal supercooled liquid, dotted lines: extrapolation of the supercooled liquid in the glassy state

tendency. Hexitols which crystallize easily (mannitol, dulcitol) are also those for which the Gibbs free energy difference (thermodynamic driving force) is expected to be the highest.

The four pentitols share the property to form a glassy state after quenching from the liquid state. Nevertheless, the glass transition temperatures are slightly different, although these compounds possess the same molecular mass [18]. We can distinguish two kinds of behaviors and group the pentitols in two pairs with respect to the value of T_g. Xylitol/adonitol exhibit a T_g at 250 K while for *l*-arabitol/*d*-arabitol, the glass transition occurs 10 K higher. These differences of behavior are also observable on the dynamic properties at the approach of T_g. The two compounds having the higher T_g are also those exhibiting the larger C_p jump amplitude and the higher fragility index. It has been shown that the deviations from the Arrhenius behavior (i.e. the fragility index value) is very often correlated to the magnitude ΔC_p of the normalized specific heat jump observed near T_g [19]. Large C_p jumps are related to a rapid decrease of the configurational entropy of the metastable liquid with regard to the equilibrium crystal when temperature decreases. This behavior indicates that slight variations of the temperature induce rapid changes of the local structure that can be related to the rapid evolutions of the dynamic. Once again, the specific molecular conformation of the different pentitols is suspected to be at the origin of the different dynamic behaviors.

* * *

This work has benefited from the help of the Nord-Pas de Calais region in the frame of the genopole program.

References

1 B. C. Hancock and G. Zografi, J. Pharm. Sci., 86 (1997) 1.
2 B. C. Hancock, S. L. Shamblin and G. Zografi, Pharm. Res., 12 (1995) 799.
3 S. L. Shamblin, X. Tang, L. Chang, B. C. Hancock and M. J. Pikal, J. Phys. Chem., 103 (1999) 4113.
4 R. Böhmer, K. L. Ngai, C. A. Angell and D. J. Plazeck, J. Chem. Phys., 99 (1993) 4201.
5 C. A. Angell, J. Res. Nat. Inst. Stand. Techn., 102 (1997) 171.
6 M. Reading, D. Elliot and V. L. Hill, J. Thermal Anal., 40 (1993) 941.
7 M. Reading, Trends Polym. Sci., 1 (1993) 248.
8 J. E. K. Shawe, Thermochim. Acta, 260 (1995) 1.
9 J. E. K. Shawe, Thermochim. Acta, 261 (1995) 183.
10 O. Bustin and M. Descamps, J. Chem. Phys., 110 (1999) 1.
11 L. Carpentier, L. Bourgeois and M. Descamps, J. Therm. Anal. Cal., 68 (2002) 727.
12 J. M. Hutchinson, Thermochim. Acta, 324 (1998) 165.
13 S. Weyer, A. Hensel and C. Schick, Termochim. Acta, 304/305 (1997) 267.
14 R. H. Doremus, Rates of phase transformations, Academic Press, New York 1985.
15 I. Gutzow and J. Schmelzer, The vitreous state, Springer, Berlin 1995.
16 P. G. Debenedetti, Metastable liquids, concepts and principles, Princeton University Press, Princeton 1996.
17 M. Siniti, J. Carre, J. M. Letoffe, J. P. Bastide and P. Claudy, Thermochim. Acta, 224 (1993) 97.
18 Y. H. Roos, Phase transitions in foods, Academic Press, New York 1995.
19 C. A. Angell, J. Non-Cryst. Solids, 131–133 (1991) 13.